Crystal structure and superconductivity of TiZr up to 57 GPa

I. O. Bashkin,[1] V. K. Fedotov,[1] M. V. Nefedova,[1] V. G. Tissen,[1] E. G. Ponyatovsky,[1] A. Schiwek,[2] and W. B. Holzapfel[2]
[1]*Institute of Solid State Physics RAS, Chernogolovka, Moscow District, 142432, Russia*
[2]*Fachbereich 6-Physik, Universität Paderborn, D-33095 Paderborn, Germany*
(Received 13 March 2003; published 1 August 2003)

The crystal structure of the equiatomic TiZr alloy is studied in the pressure range up to 57 GPa using the diamond anvils and synchrotron radiation. It is found that this alloy follows the $\alpha \rightarrow \omega \rightarrow \beta$ transition series earlier observed on Zr and Hf. Superconductivity measurements on the same alloy to 47 GPa show that the transition to the bcc β phase is connected with an increase in the superconducting transition temperature to 15 K. The pressure dependence of the atomic volume is fitted to an equation of state. Low values of the pressure derivative of the bulk modulus as well as the increase in the superconducting transition temperature are discussed in terms of a pressure-induced $s-d$ electron transfer.

DOI: 10.1103/PhysRevB.68.054401 PACS number(s): 74.62.Fj, 61.50.Ks, 61.66.Dk, 64.30.+t

I. INTRODUCTION

The interest in the high-pressure behavior of the group IV metals was revived about 12 years ago by the discovery of the hexagonal ω to the bcc β phase transitions in Zr and Hf.[1–5] These observations presented a remarkable experimental support to the theoretical ideas based on the electronic band-structure calculations for the transition metals and the calculated dependence of the electronic properties on pressure or the atomic volume.[6–9] The most important result of these calculations is the observation that the relatively narrow *d*-band moves with respect to the bottom of the broad *sp*-band when the atomic volume is varied.[6,7] This shift of the *d*-band results in a change of the *d*-band occupancy under pressure and provides the main contribution to the pressure dependence of the electronic properties of the metals (see review Ref. 6). The total band-energy calculations indicate also that the structural stability is strongly correlated with the *d*-band occupancy (Refs. 7–9, and references therein). The calculations gradually reproduced the correct structural sequence in the Periodic Table for all nonmagnetic metals at atmospheric pressure,[7–9] and the structural sequences were presented for many group I–III metals under pressure.[7,8] The high-pressure stability of the β phase in Zr and Hf has been modeled theoretically[10] parallel to the experimental observations, and the whole $\alpha \rightarrow \omega \rightarrow \beta$ transition series starting with the hcp α phase was reproduced in further theoretical studies.[11–13]

For Zr at 300 K, the $\alpha-\omega$ equilibrium pressure is 2.2 GPa,[14] and the $\omega-\beta$ transition occurs at 33 ± 2 GPa.[1–3] The equilibrium pressures for the $\alpha-\omega-\beta$ structural sequence observed in Hf are about 38 and 71 GPa, respectively.[5] Measurements of the superconducting transition temperature, T_c, in Zr under pressure show its increase by about 5 K at the $\omega-\beta$ transition.[4,15,16] Original speculations on the nature of the transition[1] relate the *d*-band occupancy critical for the structural change with the pressure-induced $s \rightarrow d$ electron transfer and with the lower partial volume of the *d*-electrons. It was also emphasized[3] that the atomic volumes and the T_c values are nearly the same for β-Zr above the structural transition and for Nb at normal pressure therefore it was assumed that the *d*-band occupancy is the same in β-Zr and in Nb under appropriate conditions. In other words, β-Zr becomes a group V element from the point of view of its structure and properties dependent on the *d*-band occupancy. Titanium shows a different behavior at very high pressures. Although the $\alpha-\omega$ equilibrium pressure is also low, 2.0 GPa at 300 K,[14] ω-Ti does not undergo a transition to the β phase up to 216 GPa.[17,18] Instead, two orthorhombic Ti phases were found with the $\omega-\gamma$ transition pressure of 116 GPa in Ref. 19 or 128 GPa in Refs. 17,18 and the $\gamma-\delta$ transition pressure of 140 GPa.[17,18] The situation for Ti is complicated for the total energy calculations as well. The calculations predict the same $\alpha-\omega-\beta$ structural sequence in Ti with the $\omega-\beta$ transition around 100 GPa therefore the orthorhombic γ and δ phases are discussed as intermediate and metastable at room temperature.[13,20,21]

The analogy between Zr and the group V metals is fraught with interesting consequences for the Zr-based alloys because alloying is a well-known means for varying the electron concentration.[6,22,23] Ti–Zr alloys are of a particular interest in this case. The $T-P$ phase diagrams of Ti and Zr are very similar up to 10 GPa.[24] Both metals undergo the $\alpha-\beta$ transition at atmospheric pressure upon heating above 1155 and 1136 K, respectively, and the $\alpha-\omega$ transition on compression. The $\alpha-\omega-\beta$ triple points are located at 913 K and 8.0 GPa for Ti (Ref. 25) and at 973 K and 5.5 GPa for Zr.[26] The $\omega-\beta$ transition lines have small positive slopes near the triple points.[24] Ti and Zr are completely soluble in their α and β phases at atmospheric pressure[27] as well as in their ω phase.[28,29] The $\alpha-\beta$ transition temperature has a minimum at 852 K at ambient pressure for the equiatomic TiZr alloy, and the parameters of the $\alpha-\omega-\beta$ triple point, 733 K and 4.9 GPa, are also lower in this case than in the pure metals.[28] The $\alpha \rightarrow \omega$ transition occurs in Ti–Zr alloys around 10 GPa at 300 K.[29,30] The superconducting transition temperatures of the α-Ti_xZr_{1-x} alloys at atmospheric pressure, $T_c(x)$, are low and reach a maximum of just 1.7 K at $x=0.5$.[31]

The analogy between Nb and β-Zr has been extended more recently to considerations on the behavior of the β-phase Ti–Zr alloys under high pressure, which should have much in common with the Ti–group V metal alloys, particularly, Ti–Nb at normal pressure.[30] The T_c measure-

ments on the Ti_xZr_{1-x} alloys with $x \leqslant 0.5$ showed discontinuities in the $T_c(P)$ curves around 10 GPa and above 30 GPa, which was attributed to the structural transitions. The isobaric $T_c(x)$ values taken at 46 GPa increased to 15 K as the Ti content increased to $x=0.5$,[30] which is rather similar to the behavior of the Ti–Nb alloys.[31] In order to complete the analogy, the present work deals with structural properties of the equiatomic TiZr alloy under pressures up to 57 GPa. X-ray diffraction is used thereby to confirm the $\alpha \rightarrow \omega \rightarrow \beta$ structural sequence, which perfectly explains then the high-pressure superconducting behavior of this alloy.

II. EXPERIMENT

The TiZr alloy was prepared from the metallic elements with total impurity contents less than 0.02 and 0.04 at.%, respectively. A Zr rod was mounted coaxially into a Ti pipe of a corresponding mass, and this assembly was subjected to multiple electron-arc melting in vacuum. The chemical composition of the final alloy was measured with an electron-microprobe, JXA-5, which showed a uniformity of ± 0.4 at.% with 49.6 at.% Ti and 50.4 at.% Zr. The lattice parameters of this (hcp) alloy were $a=310.4$ pm and $c=492.3$ pm,[28] respectively.

Energy dispersive x-ray diffraction (EDXD) experiments were performed on the F3 beamline at the HASYLAB (DESY, Hamburg).[32] Diamond-anvil cells[33,34] with flats of 0.5 mm or 0.3 mm diameter were used to generate high pressures. The samples were placed into holes in the Inconel gaskets of 0.25 or 0.15 mm, respectively, together with a few ruby chips and with white mineral oil as pressure transmitting medium. Pressure was measured with the ruby luminescence technique[35] on the basis of the nonlinear ruby scale.[36] The diffraction spectra were collected with a Ge detector at a Bragg angle of $\theta \approx 5.11°$ in typically 15 min. Two series of experiments were performed on the TiZr alloy at room temperature. The first series was a compression/decompression cycle to 38.3 GPa using the anvils with 0.5 mm flats, and the second series was a compression run to 56.9 GPa.

The superconductivity measurements used a different diamond-anvil cell made of a non-magnetic alloy with diamond flats of 0.5 mm diameter.[30] The pressure-transmitting medium was the 4:1 methanol–ethanol mixture. The superconducting transitions were recorded as jumps in the thermal dependence of the magnetic susceptibility, $\chi(T)$, measured on heating. (Cu–Fe)–Cu thermocouples were used for the temperature measurements with an accuracy of ± 0.2 K.

III. RESULTS

The $\alpha-\omega-\beta$ structural sequence includes three well-known structures that give distinctly different EDXD spectra as illustrated in Figs. 1–3. Only the α phase is observed on increasing pressure up to 10.3 GPa (Fig. 1). The α phase still predominates in the EDXD spectra at 12.2 GPa, but the onset of the $\alpha-\omega$ transition is noticeable at this pressure by small distortions of the strong α-phase reflections. The ω phase dominates in the diffraction pattern taken at 15.5 GPa and persists then up to about 54 GPa. A typical EDXD spectrum

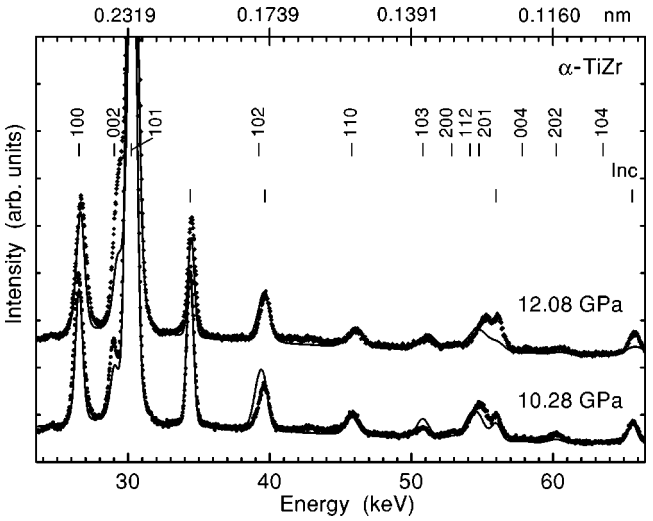

FIG. 1. Room-temperature EDXD spectra for TiZr at 10.3 GPa (bottom) and 12.1 GPa (top). Experimental data are plotted as points, and the computer-simulated patterns are represented by solid lines. Miller indices are given for the α phase at 10.3 GPa, the Inconel reflections are marked without indexing. The upper axis gives the relation between the energy scale and the interplanar spacings.

of ω-TiZr (at 39.1 GPa) is shown in Fig. 2. In the first pressure series ending at 38.3 GPa, the ω-phase was then maintained on decompression down to normal conditions.

Above 45 GPa in the second experiment, the relative intensities in the diffraction patterns start to change, and the pattern observed at the highest pressure of 56.9 GPa corresponds to pure β phase with the lattice parameter of 309.8 pm, as shown in Fig. 3. The comparison of the bar diagrams of the β and ω phases in Fig. 3 illustrates that all reflections of the β phase overlap with lines from the ω phase. This overlap results from a close relation between the ω and β structures. In fact, the ω phase is often considered as a distortion of the β phase, the central atoms of each bcc cell

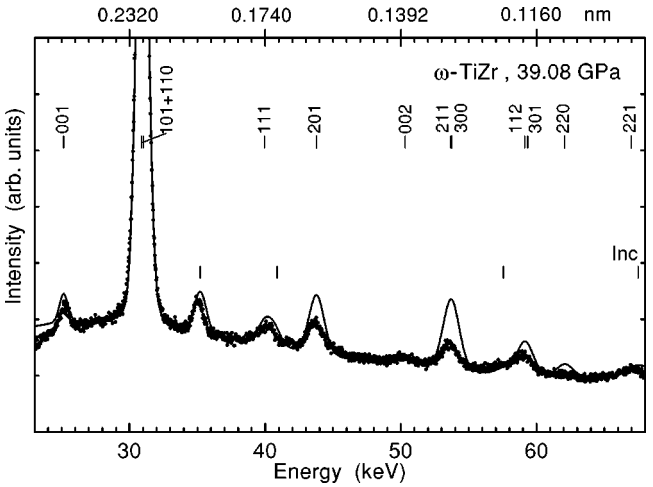

FIG. 2. Room-temperature EDXD spectrum for TiZr at 28.7 GPa. Miller indices are given for the ω phase. Other notations are the same as in Fig. 1.

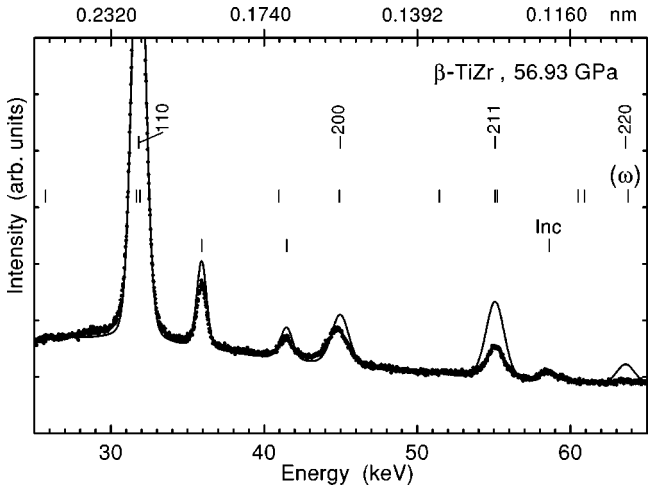

FIG. 3. Room temperature EDXD spectrum for TiZr at $P = 56.9$ GPa. Miller indices are given for the β phase. The calculated bar diagrams for ω-TiZr and for Inconel are presented without indexing. Other notations are the same as in Fig. 1.

being shifted by 1/6 along the body diagonal of this cell and the shifts in the neighboring cells being in opposite directions. Therefore the amount of the ω phase with respect to the β phase is estimated from the relative intensity of a prominent $(001)\omega$ peak with respect to the summary intensity, I_S, of the $(101)\omega+(110)\omega+(001)\beta$ peak. The pressure dependence of this relative intensity, $I(001)\omega/I_S$, in Fig. 4 illustrates the evolution of the $\omega-\beta$ transition. Obviously, the $\omega-\beta$ transition begins above 40 GPa and is completed around the final point of the present experimental region. The 50% $\omega-\beta$ conversion is obtained on this forward transition at about 52 GPa. This rather broad transition range is different from the previously observed narrow range for pure Zr,[1–4] but it is similar to the situation in Hf where this transition spans a range of the order of 10 GPa.[5]

The present structural data allow now for a detailed interpretation of the superconducting behavior reported recently[30]

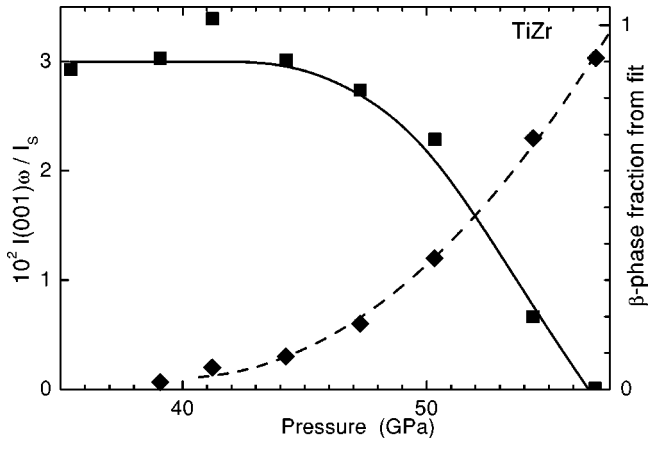

FIG. 4. Effect of pressure on the relative intensity of the $(001)\omega$ reflection with respect to the total intensity of the $(101)\omega+(110)\omega+(001)\beta$ line (squares) and the estimated variation of the relative amount of the β phase (diamonds) in TiZr at the phase transition. The lines are guides to the eyes.

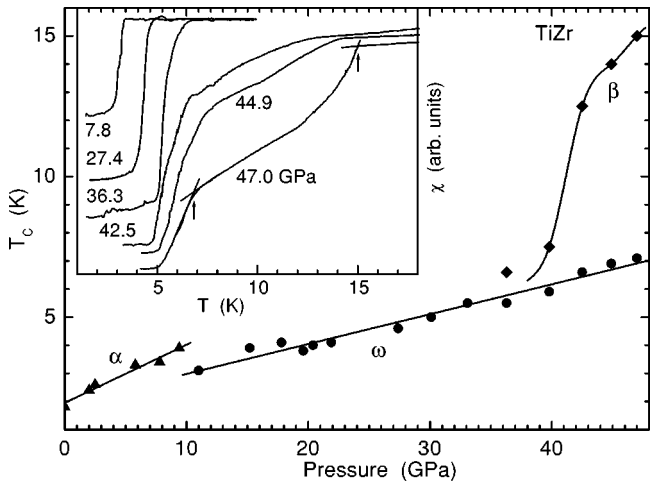

FIG. 5. Effect of pressure on the superconducting transition temperature of TiZr. Representative isobars for the magnetic susceptibility measured on heating, $\chi(T)$, are shown in the inset. Arrows in the inset mark the T_c values.

for Ti–Zr alloys under pressure. Figure 5 shows the pressure dependence of the superconducting transition temperature of the present TiZr alloy to 47 GPa. Several experimental isobars of the magnetic susceptibility, $\chi_P(T)$, are represented in the inset. The steps in the $\chi(T)$ curves are due to the superconducting transitions in the alloy. The T_c values were determined from each $\chi(T)$ curve as intersection points between the steepest tangent to the curve and the linear extension of the high-temperature section of the curve, as illustrated with arrows in Fig. 5.

Three distinctly different sections are seen in the $T_c(P)$ curve in Fig. 5. In the pressure range 0–9.4 GPa, T_c increases from 1.8 to 3.9 K. A small decrease in T_c around 10 GPa is clearly related to the $\alpha-\omega$ transition in the alloy. This value for the transition pressure compares also very well with the previous data[29] where partial $\alpha-\omega$ transitions were observed in Ti_xZr_{1-x} alloys with $x=0.74$, 0.66, and 0.56 which had been treated under quasihydrostatic pressures of about 9 GPa at room temperature. Above 11 GPa, the T_c values increase with an average slope of $dT_c/dP \approx 0.11$ K/GPa up to 36 GPa where the steps in $\chi(T)$ become less distinct (see the inset). This distortion of the superconducting anomaly finally changes into the second step in the $\chi(T)$ curves. The occurrence of two $\chi(T)$ anomalies indicates that the $\omega\rightarrow\beta$ transition proceeds through a two-phase state rather than through a gradual change of the central-atom displacements. In other words, the $\omega\rightarrow\beta$ transition proceeds directly as a first-order phase transition without any possible intermediate low-symmetry phase. The nucleation of the new superconducting high-pressure phase results in a distortion of the $\chi(T)$ anomaly, and the occurrence of the distinct second step in $\chi(T)$ at 47 GPa indicates that the amount of the β phase in the sample becomes here comparable to the amount of the ω phase. This correlates well with the EDXD data that are indicative of the 10–20% degree of the $\omega\rightarrow\beta$ transition at this pressure and room temperature. The T_c value of β-TiZr is 15 K at 47 GPa. Among the bcc metals, a higher value has been observed only for vanadium

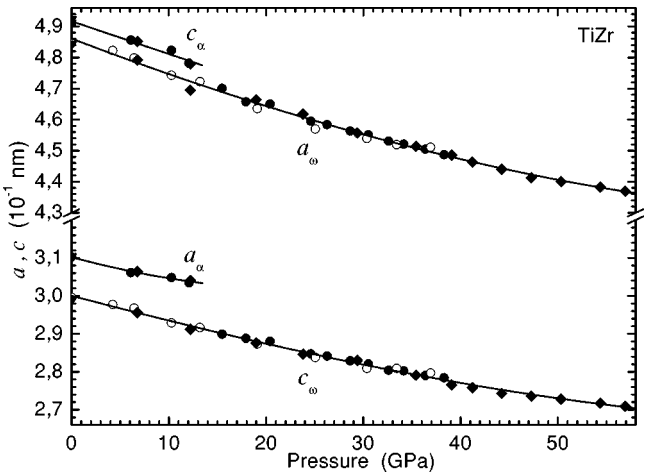

FIG. 6. Effect of pressure on the TiZr lattice parameters. Data from the first experiment are plotted as solid (compression) and open (decompression) circles, diamonds are for the second experiment. Solid lines are guides to the eye. The data at ambient pressure are taken from Ref. 28.

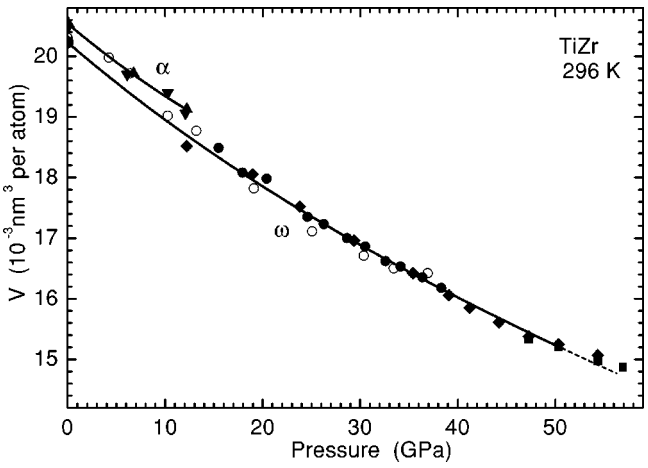

FIG. 7. Effect of pressure on the atomic volumes of the α, ω, and β phases of TiZr. Solid lines represent the fitted EOS for the α and ω phases. The experimental data for the ω phase are given by solid circles for compression and open circles for decompression in the first series and by diamonds for the second series. The α phase is represented by downward triangles in the first series and by upward triangles in the second series; squares are for the β phase in the second series. The data at ambient pressure are taken from Ref. 28.

whose T_c gradually increased to 17.2 K upon compression to 120 GPa.[37]

Comparing the experimental data on the structural and superconducting behavior, one can conclude that the TiZr alloy undergoes the $\alpha-\omega$ transition on increasing pressure at $P=11.0\pm1.5$ GPa, and the $\omega-\beta$ transition is extended on increasing pressure over a wide interval from about 43 to 57 GPa.

Further evaluation of the experimental EDXD spectra was based on a Rietveld-type simulation. A multiphase diffraction pattern including the appropriate TiZr phases and Inconel was generated for each EDXD spectrum and fitted to the spectrum with respect to the positions of the diffraction peaks. A detailed refinement including the peak intensities was not attempted for various experimental reasons, but primarily because the small number of grains in the samples could not produce an ideal powder pattern in EDXD. The quality of the fit is illustrated in Figs. 1–3, where the experimental data are represented with points, the solid lines are the simulated diffraction patterns, and the calculated peak positions are shown with bars. Figure 6 presents the pressure dependence of the corresponding lattice parameters a and c for the α and ω phases. The ratios of the lattice parameters of the ω phase, $c/a=0.618\pm0.002$, and of the α phase, $c/a=1.581\pm0.005$, are the same within the experimental accuracy for all points in Fig. 6 and agree very well with the data for atmospheric pressure, $c/a=0.617$ and 1.586, respectively.[28] This constancy of c/a is similar to the situation in α- and ω-Zr.[1] The amount of the β phase in the region of the $\omega-\beta$ transition estimated using this data treatment is compared with the decreasing intensity of the $(001)\omega$ reflection in Fig. 4.

Figure 7 shows the effect of pressure on the average atomic volume, $V(P)$. Solid lines in Fig. 7 represent fits of the $V(P)$ data for the α and ω phases by the use of an equation of state (EOS) in the form of an adapted polynomial expansion previously labeled AP2,[38]

$$P=3\cdot K_0\cdot x^{-5}\cdot(1-x)\cdot(1+c_2x(1-x))\cdot e^{c_0(1-x)}.$$

Here $x=(V/V_0)^{1/3}$, V_0 is the average atomic volume, and K_0 is the isothermal bulk modulus, both at ambient pressure. Model constant $c_0=-\ln(3\cdot K_0/P_{\mathrm{FG}_0})$ compares K_0 with the pressure of a Fermi gas, $P_{\mathrm{FG}_0}=a_{\mathrm{FG}}(Z/V_0)^{5/3}$, for the average electron density, Z/V_0, where Z stands for the average number of electrons per atom and $a_{\mathrm{FG}}=23.37\cdot10^{12}$ GPa$\cdot$pm^5 is a universal constant. For regular solids c_2 is a small correction related to $K_0'=3+(2/3)(c_0+c_2)$. This EOS is favored here because it includes the correct asymptotic behavior under very strong compression. A detailed discussion of the advantages of the AP2 form has been given elsewhere.[38]

The average atomic volumes of the α- and ω-TiZr phases at atmospheric pressure have been determined previously:[28] $V_{0\alpha}=20.539\cdot10^6$ pm^3 and $V_{0\omega}=20.231\cdot10^6$ pm^3. Values for K_0 and K_0' from the present AP2 fitting are listed in Table I. For the present moderate ranges in pressure, the choice of the EOS form does not affect noticeably the values of K_0 and K_0', which allows comparing the present data with previous values for pure Ti and Zr metals although different EOS forms had been used in these data evaluations. A remarkable feature of all these evaluations are very low values of the pressure derivative of the bulk modulus, K_0', for all the phases involved.

The volume decrease at the $\alpha-\omega$ transition in the TiZr alloy at 11 GPa is found to be $\Delta V=0.44\cdot10^6$ pm^3/atom or $\Delta V/V_{0\alpha}=2.1\%$. The volume decrease at the $\omega-\beta$ transition in the TiZr alloy derived from four EDXD spectra between 47.3–56.9 GPa is roughly $0.065\cdot10^6$ pm^3/atom, or 0.3%. While the volume decrease at the $\alpha-\omega$ transition is comparable to the values for Ti and Zr, the present value for the

TABLE I. Atomic volumes, isothermal bulk modulus, K_0, and pressure derivatives, K_0', for the α and ω phases of TiZr and the corresponding values for elemental Ti and Zr. The numbers in parentheses represent standard deviations of the last digit from the fits only. The additional uncertainties for the K_0' values due to uncertainties in the ruby scale are probably 0.3.

	V_0 (10^6 pm^3)	K_0 (GPa)	K_0'	Ref.
α-Ti	17.735	102	9.1	19
α-TiZr	20.539	148(3)	3.8(2)	Present
ω-Ti	17.37	142	2.3	19
ω-Ti	17.37	123.1	3.2	17,18
ω-TiZr	20.231	146(3)	1.7(2)	Present
ω-Zr	. . .	104	2.1	1
ω-Zr	22.7	121	1.7	3
β-Zr	18.0	201	0.8	3
γ-Ti	17.05	152	2.0	19

volume decrease at the $\omega-\beta$ transition is very small compared to the values reported for pure Zr and pure Hf, as shown in Table II.

IV. DISCUSSION

The strongly reduced value of $\Delta V/V$ for the $\omega-\beta$ transition in TiZr with respect to pure Zr is a remarkable feature. This implies that further increase in the Ti content can result in the opposite sign of the volume effect. In other words, one expects that the $\omega-\beta$ transition pressure rapidly increases with increasing Ti content, and this trend gives also a thermodynamic reason for the observation of a different transition, $\omega-\gamma$, with $\Delta V/V=-1.6\%$[17–19] in pure titanium.

Another remarkable feature is presented as very low values for the pressure derivative of the bulk modulus, K_0', for all phases of the group IV metals in Table I (with the exception of the value for α-Ti which seems doubtful). This observation was made earlier[39] and related there to the pressure-induced $s\rightarrow d$ electron transfer at the beginning of the transition metal series compared to the middle of the transition metal series where $K_0'\approx 5$. The data in Table I indicate therefore that the $s\rightarrow d$ electron transfer in the group IV metals is not only responsible for the structural transitions, but also for the anomalies in the EOS shown by the low K_0' values. The change in the *d*-band occupancy at the structural transitions should therefore be small, much less than one electron per atom, explaining also the relatively small values for the volume decrease at these phase transitions. There are some theoretical estimates (e.g., Ref. 8) that the bcc structure becomes stable in the early transition metals when the total number of the valence electrons per atom, *z*, becomes larger than 4.2, or the number of the *d*-electrons becomes $N_d>2.2$. These theoretical numbers correlate with the experimental observation that the bcc solid solutions are stable in many group IV–V metal alloys at normal pressure when the concentration of the group V metal becomes larger than about 25%.[27,31] One may conclude therefore that the *d*-band occupancy directly after the transition to the β phase is also still considerably less than 3.

TABLE II. Volume decrease and transition pressures, P_{tr}, for the group IV metals together with the present data for TiZr. Arrows represent values for the forward transitions only.

Transition	Metal	$\Delta V/V$ (%)	P_{tr} (GPa)	Ref.
	Ti	1.4 to 1.7	2.0	24
$\alpha-\omega$	Zr	2.3	2.2	24
	Hf	0.54	38	5
$\alpha\rightarrow\omega$	Ti	1.9	9	19
	TiZr	2.1	11 ± 1.5	present
$\omega-\beta$	Zr	1.6	30	1
	Hf	2.1	71	5
$\omega\rightarrow\beta$	Zr	1.8	33	3
	TiZr	0.3	43 to 57	present
$\omega-\gamma$	Ti	1.6	116	19
$\omega\rightarrow\gamma$	Ti	1.6	128	17,18
$\gamma\rightarrow\delta$	Ti	1.4	140	17,18

Superconducting transition temperatures as well as many other electronic properties and their systematics in the Periodic Table are commonly discussed in the framework of the empirical rigid band models related to the Matthias rule.[22,23,31] The basic idea is that the metallic properties depend on the electronic density of the states at the Fermi level, N_F, and its dependence on the total concentration of the valence electrons, *z*, with the assumption that the $N_F(z)$ curve is the same for all metals with the same[22,31] or even different[23] crystal structures in each metal series of the Periodic Table. The experimental and theoretical high-pressure data presently available show deviations from this simple rule. Theoretical determinations of the electronic density-of-states (DOS) spectra for three Zr phases at different pressures[11] indicate that the relative positions of the *s*- and *d*-bands and the shapes of the DOS curves are pressure-dependent. The total number of the valence electrons cannot change at the phase transitions in the group IV metals and alloys, but T_c can increase by an order of magnitude in the experimental pressure range. There is a strong concentration dependence of T_c in the β-Ti_xZr_{1-x} alloys at a constant pressure[30] as in many group IV–V metal alloys, but *z* has the same value for any concentration in the Ti–Zr alloys. Furthermore, the T_c pressure dependence, dT_c/dP, above the $\omega-\beta$ transition is also concentration dependent.[30] These observations are not consistent with the Matthias rule but can be readily understood if one admits that the electronic and structural properties of the transition metals are primarily dependent on the number of *d*-electrons, N_d, and not so closely related to the total number of valence electrons, *z*.

V. CONCLUSIONS

The present structural study on the equiatomic TiZr alloy under high pressure confirms the expected $\alpha\rightarrow\omega\rightarrow\beta$ structural sequence with average forward transition pressures of about 11 and 52 GPa, respectively. The volume decrease at the $\omega-\beta$ transition in TiZr is small compared to this value for Zr, which relates well to the observation that this transi-

tion may occur in pure Ti only at much higher pressures or not at all. The EOS for TiZr is characterized by a low value for the pressure derivative of the bulk modulus, K_0'. This softness in the equation of state is typical for a pressure-induced $s-d$ electron transfer. The transition to the bcc β-TiZr phase is connected with an increase in the superconducting transition temperature from 6 to 15 K. The variations in the superconducting properties are well understood on the basis of pressure-dependent shifts of the Fermi level within the *d*-band.

ACKNOWLEDGMENTS

X-ray studies were performed under Project No. II-96-76. The Russian group was supported by the RFBR Grant No. 00-02-17562 and by the RAS program ''Physics and chemistry of the extreme states of the matter.''

[1] H. Xia, S.J. Duclos, A.L. Ruoff, and Y.K. Vohra, Phys. Rev. Lett. **64**, 204 (1990).
[2] H. Xia, A.L. Ruoff, and Y.K. Vohra, Phys. Rev. B **44**, 10 374 (1991).
[3] Y. Akahama, M. Kobayashi, and H. Kawamura, J. Phys. Soc. Jpn. **60**, 3211 (1991).
[4] Y. Akahama, M. Kobayashi, and H. Kawamura, J. Phys. Soc. Jpn. **59**, 3843 (1990).
[5] H. Xia, G. Parthasarathy, H. Luo, Y.K. Vohra, and A.L. Ruoff, Phys. Rev. B **42**, 6736 (1990).
[6] I.V. Svechkarev and A.S. Panfilov, Phys. Status Solidi B **63**, 11 (1974).
[7] J.C. Duthie and D.G. Pettifor, Phys. Rev. Lett. **38**, 564 (1977).
[8] H.L. Skriver, Phys. Rev. B **31**, 1909 (1985).
[9] M. Sigalas, D.A. Papaconstantopoulos, and N.C. Bacalis, Phys. Rev. B **45**, 5777 (1992).
[10] J.S. Gyanchandani, S.C. Gupta, S.K. Sikka, and R. Chidambaram, J. Phys.: Condens. Matter **2**, 6457 (1990).
[11] R. Ahuja, J.M. Wills, B. Johansson, and O. Eriksson, Phys. Rev. B **48**, 16 269 (1993).
[12] S.A. Ostanin and V.Yu. Trubitsin, Phys. Rev. B **57**, 13 485 (1998).
[13] K.D. Joshi, G. Jyoti, S.C. Gupta, and S.K. Sikka, J. Phys.: Condens. Matter **14**, 10921 (2002).
[14] V.A. Zilbershtein, N.P. Chistotina, A.A. Zharov, N.S. Grishina, and E.I. Estrin, Fiz. Met. Metalloved. **39**, 445 (1975).
[15] Y. Akahama, M. Kobayashi, and H. Kawamura, High Press. Res. **10**, 711 (1992).
[16] I.O. Bashkin, M.V. Nefedova, and V.G. Tissen, Phys. Solid State **42**, 11 (2000).
[17] Y. Akahama, H. Kawamura, and T. LeBihan, J. Phys.: Condens. Matter **14**, 10583 (2002).
[18] Y. Akahama, H. Kawamura, and T. Le Bihan, Phys. Rev. Lett. **87**, 275503 (2001).
[19] Y.K. Vohra and P.T. Spencer, Phys. Rev. Lett. **86**, 3068 (2001).
[20] J. S. Gyanchandani, S. K. Sikka, and R. Chidambaram, in *Proceedings of the International Conference on High Pressure Science and Technology, Bangalore, 1991* (Oxford, New Delhi, 1992), p. 331.
[21] K.D. Joshi, G. Jyoti, S.C. Gupta, and S.K. Sikka, Phys. Rev. B **65**, 052106 (2002).
[22] G. Gladstone, M. A. Jensen, and J. R. Schrieffer, *Superconductivity in the Transition Metals: Theory and Experiment, in Superconductivity*, edited by R. D. Parks (Marcel Dekker, New York, 1969).
[23] A.R. Miedema, J. Phys. F: Met. Phys. **4**, 120 (1974).
[24] E. Yu. Tonkov, *High Pressure Phase Transformations* (Gordon and Breach, Philadelphia, 1992) Vol. 2, pp. 682, 691.
[25] F. P. Bundy, in *New Materials and Methods for Investigation of Metals and Alloys* (Metallurgia, Moscow, 1966), p. 230; G. E. Research Laboratory Report No. 63-RL-348IC, October 1963, USA.
[26] A. Jayaraman, W. Klement, and G.C. Kennedy, Phys. Rev. **131**, 644 (1963).
[27] M. Hansen and K. Anderko, *Constitution of Binary Alloys* (McGraw–Hill, New York, 1958), Vol. 2; F. A. Shunk, *Constitution of Binary Alloys, Second Supplement* (McGraw–Hill, New York, 1967).
[28] I.O. Bashkin, A.Yu. Pagnuev, A.F. Gurov, V.K. Fedotov, G.E. Abrosimova, and E.G. Ponyatovskii, Phys. Solid State **42**, 170 (2000).
[29] V.V. Aksenenkov, V.D. Blank, B.A. Kulnitskii, and E.I. Estrin, Fiz. Met. Metalloved. **69**, 154 (1990).
[30] I.O. Bashkin, V.G. Tissen, M.V. Nefedova, A. Schiwek, W.B. Holzapfel, and E.G. Ponyatovsky, JETP Lett. **73**, 75 (2001).
[31] E. M. Savitskii, Yu. V. Efimov, N. D. Kozlova, B. P. Mihailov, L. F. Myzenkova, and E. D. Doronkin, *Superconducting Materials* (Metallurgia, Moscow, 1976).
[32] J.W. Otto, Nucl. Instrum. Methods Phys. Res. A **384**, 552 (1996).
[33] K. Syassen and W.B. Holzapfel, Europhys. Conf. Abstr. **1A**, 75 (1975).
[34] W. B. Holzapfel, in *High Pressure Chemistry*, edited by H. Kelm (Reidel, Boston, 1978), p. 177.
[35] R.A. Forman, G.J. Piermarini, J.D. Barnett, and S. Block, Science **176**, 284 (1972); G.J. Piermarini, S. Block, and J.D. Barnett, J. Appl. Phys. **44**, 5377 (1973).
[36] H.K. Mao, P.M. Bell, J.W. Shaner, and D.J. Steinberg, J. Appl. Phys. **49**, 3276 (1978).
[37] M. Ishizuka, M. Iketani, and S. Endo, Phys. Rev. B **61**, R3823 (2000).
[38] W.B. Holzapfel, Z. Kristallogr. **216**, 473 (2001).
[39] Y.K. Vohra, S.K. Sikka, and W.B. Holzapfel, J. Phys. F: Met. Phys. **13**, L107 (1983).